Report 16, 1993

GEOTHERMOMETRY AND MINERAL EQUILIBRIA OF THERMAL WATERS FROM THE GUANZHONG BASIN, CHINA

Zheng Xilai,
UNU Geothermal Training Programme,
Orkustofnun - National Energy Authority,
Grensasvegur 9,
108 Reykjavik,
ICELAND

Permanent address:
Department of Hydrogeology and Engineering Geology,
Xi'an College of Geology,
Xi'an 710054,
P.R. CHINA

Report 16, 1993

ABSTRACT

This report describes the regional geotectonic and geothermal features to present a conceptual model of the thermal activity in the Guanzhong basin, China, and reviews the most important methods of geothermal sampling and chemical analysis used in China. Silica and cation geothermometers are applied to predict possible subsurface temperatures using chemical analytical data calibrated by chemical equilibrium calculations with the chemical speciation programme WATCH. In order to further confirm the reliability of the geothermometer temperatures, a great effort is made to study the equilibrium state of thermal waters by means of log Q/K diagram, Na-K-Mg triangular diagram and by studying the equilibrium state of some species at the chalcedony and quartz reference temperatures. Finally, the possible subsurface temperatures are predicted in the scattered thermally anomalous areas after a careful consideration of the equilibrium state of all the water samples.

The studies of aqueous chemistry in the Guanzhong basin show that the use of geothermometry is conditional. In other words, physical processes like conductive cooling, mixing with cold water and boiling during upflow may affect possible water-rock equilibria in the deep reservoir, and this can result in unreliable temperature predictions. Furthermore, it is very useful to employ different geothermometers and methods for the studies of equilibrium state to check each and to exclude the unreliable samples.

TABLE OF CONTENTS

LIST OF FIGURES

LIST OF TABLES

1. INTRODUCTION

The Guangzhong basin in the drainage area of Yellow river is one of the earliest settling regions of the Chinese. The fossils of the famous Lantian ape-men, about 70 million years old, were found in the Lantian county, and Xi'an, now the capital of Shaanxi province, was the old capital of China for 11 dynasties lasting over 1000 years. In the Guanzhong basin the geothermal water from the Huaqing pool has been used for health spas for more than 1000 years. At present, about 20 geothermal boreholes have been drilled for space heating in Xi'an and for fish farming in an area of 335,000 m^2 in the Chang'an county, where a project aimed at increasing the water surface by 200,000 m^2 for the same purpose is under way, so the geothermal exploitation and utilization in Xi'an are at an early stage due to technical and economic problems.

Geochemistry is one of the most economical and efficient methods of studying geothermal reservoirs during exploration, exploitation and utilization. Chemical composition of hot water has proved very useful for estimating subsurface temperature, determining water origin, observing the degree of mixing and predicting possible scaling and corrosion. In other words, during the exploration stage the chemistry of the fluids can be used to indicate the subsurface temperature and the exploitation potential of the thermal system, and monitoring the chemistry of the fluids during exploitation is very important for the prediction of potential scaling, corrosion and changes in the system. Therefore, chemical composition is monitored continuously in almost all geothermal fields as well as temperature, pressure and flowrate.

This report is written as a part of my six months geothermal training at the United Nations University in Reykjavik, Iceland. Although geothermal sampling and analytical methods were studied in the field and at Orkustofnun (The National Energy Authority), Iceland, all the data used in the report were obtained from China. The programme WATCH (Arnorsson et al., 1982, Arnorsson and Bjarnason, 1993) is used to process the original analytical data for the application of geothermometry on the basis of chemical equilibrium.

2. GEOTECTONIC AND GEOTHERMAL FEATURES OF GUANZHONG BASIN

The Guanzhong basin is located in the middle of Shaanxi province, China with a semi-arid climate, an annual mean precipitation of 648.3 mm and an annual average atmospheric temperature of 13.6°C. The capital of Shaanxi province, Xi'an, lies in the centre of the basin. Weihe river passes through the basin from west to east. In addition, many branches flow from mountainous areas to the Weihe river (Figure 1). The basin can be divided into three main geomorphic units, Weihe river terraces, loess platforms and mountainous districts. Three-stage terraces, extending along the Weihe river, are found in the lowest part of the basin, but are missing in some areas due to lateral erosion by the Weihe river. Discontinuous asymmetric loess platforms are found on both sides of the terraces due to erosion by the Weihe river and its branches. Furthermore, the sharp Qinling mountain and the flat North mountain constitute the southern and northern boundaries of the basin. Liu (1975) reviewed the geotectonic features and geothermal activity in the Guanzhong basin.

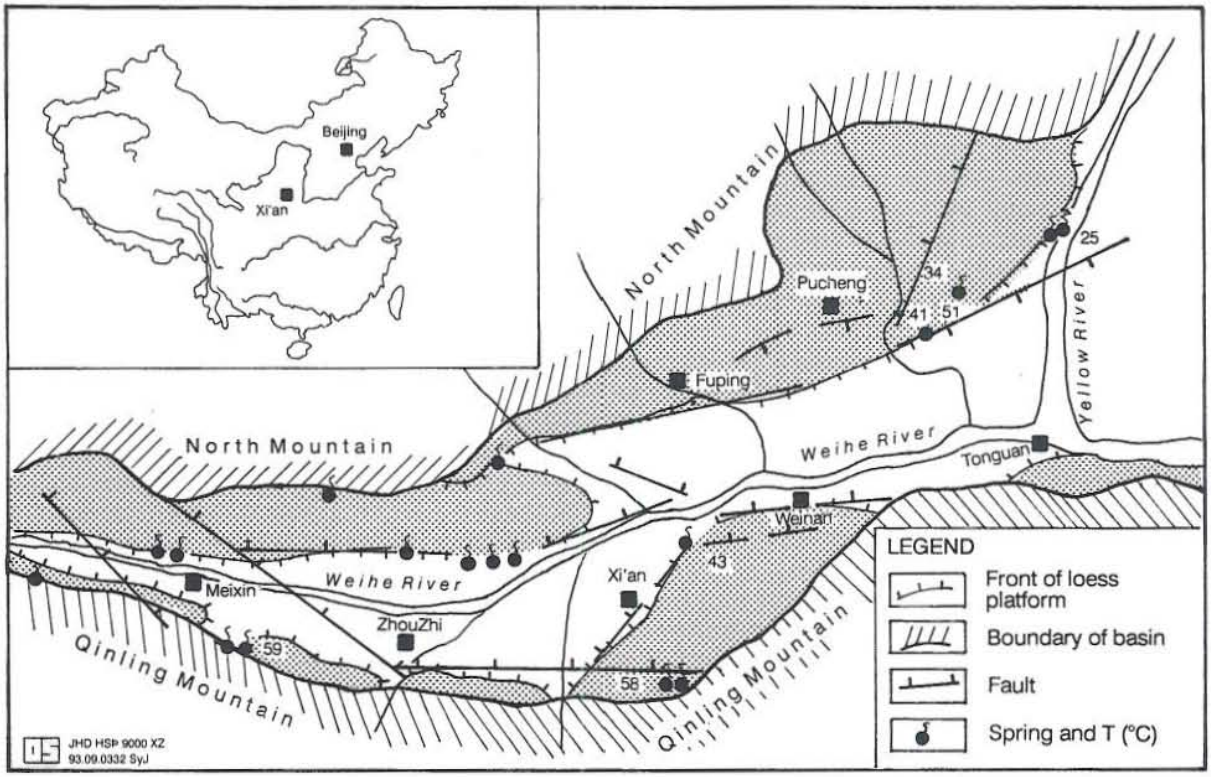

FIGURE 1: Geotectonic map of the Guanzhong basin

2.1 Strata

The Weihe river terraces, covering the bedrock, consist of Quaternary friable deposits and Tertiary river-lake deposits. The Quaternary deposits include gravel, sand, fine sand and various kinds of clay about 638 m thick. The Tertiary formations are sandy rock, fine sandy rock and argillaceous rock, etc., which constitute the major geothermal formations exploited at present, with a thickness of over 1400 m. Loess platforms, covering the bedrock and the Tertiary formations, are characterized by Quaternary aeolian soil, including several layers of ancient soil and calcic nodules, with a thickness of hundreds of meters. Generally speaking, the loess deposit is of a low permeability, and the vertical fissures in it make its permeability anisotropic. Rocks in the mountainous areas and bedrock in the basin are built of Archaean and Proterozoic metamorphic rocks, lower Palaeozoic carbonates, as well as upper Palaeozoic and Mesozoic clastic rocks and intrusive granite at different times.

2.2 Tectonic setting

The Guanzhong basin (Figures 1 and 2), known as the Weihe river graben in tectonics, extends from Baoji to the Fen river graben in Shaanxi province. The northern and southern borders of the basin are controlled by eastnortheasterly and/or easterly trending faults forming an asymmetric graben. The boundary's tectonic outline and inner tectonics of the graben are created by the Qinling E-W trending tectonic zone, the Xinhuaxia tectonic system, the Longxi tectonic system and the Qilü arcuate folding zone. The Qinling E-W trending tectonic zone was repeatedly influenced by extensive tectonic activity up to the late Mesozoic era when the last event occurred following granite intrusions. All the earlier activity took place in the late Mesozoic era, and the events influenced one another. The Weihe river graben was formed as a result of this tectonic activity, so there are a lot of folds, faults and fissures constituting channels for geothermal waters. Furthermore, the active tectonic systems, especially the Qilü arcuate folding zone, control the distribution of earthquake epicentres. Earthquakes usually occur in the overlapping parts of the Xinhuaxia and the Qilü arcuate tectonic systems. For example, both the Huaxian earthquake of estimated intensity 8 (1556) and the Chaoyi earthquake of estimated intensity 7 (1501) on Richter scale, took place along this zone.

2.3 Geothermal activity

The Huaqing Pool (S3) in Lintong county, about 30 km from Xi'an, has been in use for bathing for over 1000 years. The East Tangyu and West Tangyu Pools (S1 and S8) are both used for bathing as a treatment for several kinds of diseases (Figure 2). In addition, geothermal water is utilized for fish farming over an area of 335,000 m^2 in Chang'an County, where a project on increasing the surface water area by 200,000 m^2 for the same purpose is under way.

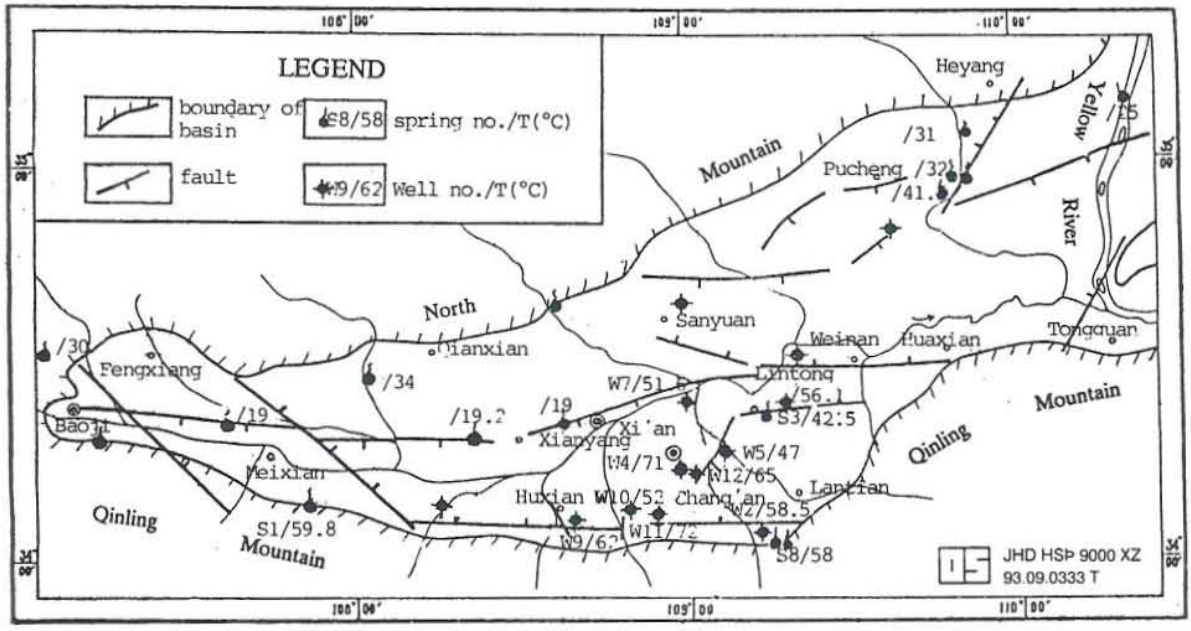

FIGURE 2: Location map of hot springs and wells in the Guanzhong basin

In general, the geothermal anomalies, which are controlled by faults in the Guanzhong basin, are discontinuous. Different heat sources, origins, flow characteristics and chemical composition complicate geothermal studies. In my opinion, the geothermal manifestations including hot

springs and boreholes occurred mainly in the following three areas: the contact zone of the Qinling mountain and the basin; the loess platform fronts and the exploited geothermal area in Xi'an and Chang'an county.

The contact zone of Qinling and the basin is a typical thermally anomalous area where the springs S1, S3, and S8 appear on the surface along the faults at the foot of the Qinling mountain. The deep faults formed by the repeated intensive tectonic activity permit cold water to enter deep crust, and then return to shallow aquifers or reach the surface along the faults at some favourable spots after it is heated by the deep heat source (Figure 2). The loess platform fronts are often fault lines which can constitute discharge channels for geothermal water, so many warm springs with temperatures of 20-40°C issue from them. At present, the springs have not been utilized because of their low temperatures, so all the samples used in the report are from the other two areas.

The two areas mentioned above are far away from the major industrial city Xi'an. In addition, about ten geothermal boreholes with depths of 1000-2000 m have been drilled in Xi'an, and several hot wells (350-1700 m) in Chang'an county mainly for fish farming. Furthermore, several thermal wells are scattered around the basin. All the geothermal wells are along faults or at the junctions of two or more faults. Their various temperatures (Figure 2) and chemical composition show that the hot water is from different sources, or at least different discharge channels.

3. GEOTHERMAL SAMPLING AND CHEMICAL ANALYSIS

3.1 Field sampling

The collection of representative samples from geothermal wells and springs is a complex procedure due to possible chemical precipitation, degassing, phase changes and contamination. In this area, there is no boiling water on the surface, making the sampling relatively easy. Hot water samples can be collected not only from spring mouths or wellheads but also downhole. Great care should be taken to treat samples so as to protect them from possible chemical precipitation and degassing with decrease of temperature and pressure. Some methods of treatment are presented in Table 1. For example, the water sample should be diluted on site with deionized water to bring SiO_2 below 100 ppm, and 1 ml 0.2M Zn-acetate solution has to be added to a 100 ml sample if H_2S is detectable. In addition, water samples are filtered, and 100 ml acidified with 0.2 ml concentrated HCl for Ca, Mg, Na, K analysis, and filtered, acidified with 0.2 ml concentrated HNO_3 to 100 ml for Fe, Al, Li, Rb, Cs. Treatment is not necessary before analysis of other constituents, except that muddy samples need to be filtered. Furthermore, all the containers, pipes and so on used for sampling should be cleaned by tap water, distilled water in the laboratory and by water samples from the field. Several geothermal sampling techniques have been described by Olafsson (1988).

TABLE 1: Treatment of and analytical methods for geothermal water samples in China

Component	Sample treatment	Analytical method
SiO_2	Dilution	Colorimetric with ammonium molybdate
Na, K	none	Flame photometry or AAS
Ca, Mg	Acidification	Titration with EDTA; or AAS
Fe, Al, Li	Filtration, acidification	Atomic absorption spectrophotometry (AAS)
pH, CO_2	none	Titration with HCl using pH-meter
Cl	none	Mohr titration with $AgNO_3$
SO_4	Acidification	Titration with benzidine chloride
F	none	Colorimetric with zirconium alizarin
B	none	Colorimetric with quinalizarin
H_2S	none	Iodine addition & back-titration with $Na_2S_2O_3$
Sr	Filtration, acidification	DCP or ICP emission spectrography

3.2 Laboratory analysis

The analytical techniques used in China for determining the major components in geothermal waters are summarized in Table 1. Most of the chemical data on hot waters used in the report (Table 2) were obtained by the Chemical Laboratories of Shaanxi Geological and Mineral Bureau and the Chemical Laboratory of the First Team of Hydrogeology and Engineering Geology.

TABLE 2: Chemical composition of thermal waters (ppm) from Guanzhong basin

No.	pH lab.	T (°C)	Na	K	Ca	Mg	Cl	SO_4	CO_2	F	Br	SiO_2	TDS
S1	8.30	60	145.1	7.5	9.0	0.0	21.3	236.3	57.2	20.0	0.2	75.0	566
W2	8.90	53	166.9	8.6	13.0	0.0	24.8	314.6	35.6	14.0	0.2	70.0	634
W7	8.33	61	2580.0	12.9	167.0	31.2	2140.0	3000.0	209.9	2.3	13.4	30.1	8362
S8	8.60	59	147.3	7.7	19.0	0.1	24.8	257.0	52.8	7.0	/	56.3	/
W9	8.60	62	223.0	2.2	6.0	0.2	156.0	40.8	202.4	10.7	/	53.6	768
W10	8.50	52	156.2*		9.0	0.6	42.5	206.5	73.7	/	/	29.5	520
W11	8.70	72	108.7*		7.0	0.0	23.4	115.3	83.6	/	/	26.0	/
W12	8.40	65	641.0	3.5	17.2	2.9	349.0	838.0	142.1	4.8	/	36.7	2075
S3	7.50	43	187.3	8.4	40.1	3.6	128.7	217.6	152.2	5.6	0.2	38.3	782
W4	8.50	64	875.6*		29.7	3.5	287.2	1304.0	193.6	4.5	1.5	50.0	2756
W5	8.70	47	638.7*		26.1	6.7	117.0	920.3	287.7	2.8	/	24.0	2022

* Na + K

4. PREDICTION OF SUBSURFACE TEMPERATURES

4.1 Outline

Geothermometers may be broadly classified into two groups: (1) those which are based on temperature-dependent variations in the solubility of individual minerals, and (2) those which are based on temperature-dependent exchange reactions which fix the ratios between certain dissolved constituents.

The earliest attempts to use water composition to estimate subsurface temperatures in geothermal systems date back to about 1960. Thus, Ellis and Wilson (1960) used Na/K ratios in waters at Wairakei to locate hot upflow zones. Bodvarsson and Palmason (1961) developed an empirical silica geothermometer based on the relation between silica concentrations in hot springs and reservoir temperatures in Iceland. Fournier and Rowe (1966) also used silica concentrations in well discharges and springs to estimate subsurface temperatures. In addition, Fournier and Truesdell (1973) developed an empirical Na-K-Ca geothermometer which was later extended by Fournier and Potter (1979) to include magnesium. Fouillac and Michard (1981) developed an empirical solute geothermometer based on Na/Li ratios and presented two temperature functions, one of which is applicable to low salinity waters and the other to brines. Arnorsson et al. (1982, 1983a, b) reviewed the basis of chemical geothermometry, and presented and tested several geothermometers in Icelandic geothermal systems. Arnorsson and Gunnlaugsson (1985) developed geothermometers based on the concentrations of CO_2, H_2S, and H_2 in geothermal steam and the ratios between them. These can be quite useful, especially where surface manifestations are confined to steam but are limited by subsidiary processes such as condensation and re-equilibration at decreasing temperatures. D'Amore and Panichi (1980) developed a geothermometer based on various ratios between CO_2, H_2S, H_2, CH_4 and the partial pressure of CO_2 in the system. Darling and Talbot (1992) have proposed a geothermometer which is based on CH_4/C_2H_6 ratios, which looks promising, but has not yet been widely tested. Furthermore, several isotope geothermometers have been developed.

One of the major applications of geochemistry in the exploration for geothermal resources is the prediction of subsurface temperatures using chemical geothermometers. In upflow zones below hot springs and the bottom of shallow boreholes, the water may cool due to conduction, boiling and/or mixing with cold water. With the aid of solute geothermometry and mixing models, it is possible to evaluate temperatures in the geothermal reservoirs at depths below cooling zones, using data on the chemical composition of water from hot springs and shallow boreholes. The calculation of geothermal reservoir temperatures from the chemical composition of springs and drillholes involves various assumptions and simplifications. The basic assumption is that a temperature-dependent equilibrium is attained in the geothermal reservoir between specific solute(s)/gas(es) and minerals. It is further assumed that the respective solutes or gas concentrations are not affected by chemical reactions in the upflow where cooling occurs.

4.2 Calibration of concentrations

Prediction of subsurface temperatures by chemical geothermometry often ignores the formation of complexes between solutes and assumes that analytical concentrations are equal to the activities of the aqueous species. For example, in the application of silica geothermometers analyzed aqueous silica concentrations are considered to be equal to the activity of the $H_4SiO_4^\circ$ species. Computer programmes for the calculation of aqueous speciation tend to circumvent such approximations unless the calibration of the geothermometers is based on analytical

concentrations. On the other hand, the concentration ratios of Na/K are generally very similar to the Na^+/K^+ ratio because these ions are the only significant Na and K species formed in most natural waters and have similar activity coefficients. The quartz and chalcedony solubility curves, on which the silica geothermometers are based, assume equilibrium between the $H_4SiO_4°$ aqueous species and the respective solids. Correction is very important for dilute water at a high pH. The analyzed silica expressed as SiO_2 consists mainly of the two species:

$$SiO_2(tot) = H_4SiO_4^o + H_3SiO_4^- \quad (1)$$

The relative concentrations are controlled by the reaction:

$$H_4SiO_4^o = H^+ + H_3SiO_4^- \quad (2)$$

Assuming that concentration is equal to activity, we obtain:

$$\frac{(H_3SiO_4^-)}{(H_4SiO_4^o)} = \frac{K_{diss}}{(H^+)} \quad (3)$$

The concentration of $H_4SiO_4°$ can easily be calculated by merging (1) with (3):

$$H_4SiO_4^o = \frac{SiO_2(tot)}{\frac{K_{diss}}{(H^+)} + 1} \quad (4)$$

K_{diss} is a constant at a certain temperature, so increasing pH, which means decreasing $[H^+]$, results in the decrease of the $H_4SiO_4°$ species. Generally, in cases where pH is lower than 8.5, correction is not needed for ionized silica and can be ignored. Some low-temperature geothermal waters have a pH between about 9 and 10. For such waters the approximation to take analyzed silica to represent $H_4SiO_4°$ is unsatisfactory. A substantial fraction of the silica is in the form of $H_3SiO_4^-$. The chemical speciation of thermal waters can be calculated by WATCH (Arnorsson et al., 1982, Arnorsson and Bjarnason, 1993). The programme is described briefly below.

Input to the programme is a component analysis of geothermal water at the surface, and in addition the pH temperature, and a reference temperature at which the composition is to be calculated. The concentrations of the 69 species considered in the programme are expressed in terms of the component concentrations by mass balance equations, and the chemical equilibria between the species are expressed as mass action equations. The two sets of equations are solved simultaneously by an iterative procedure. An initial estimate of the ionic strength of the water is obtained using only the concentrations of the major cations. This ionic strength is used to compute the activity coefficients using the extended Debye-Hückel formula. At last, we can easily calculate the pH, aqueous speciation, partial pressures of gases, redox potentials, and activity products by computer iteration so as to obtain the species used in geothermometry (Appendix I).

4.3 Silica geothermometry

The solubilities of several silica minerals have been determined experimentally as functions of temperature at the vapour pressure of the solution. Pressure and added salt have little effect

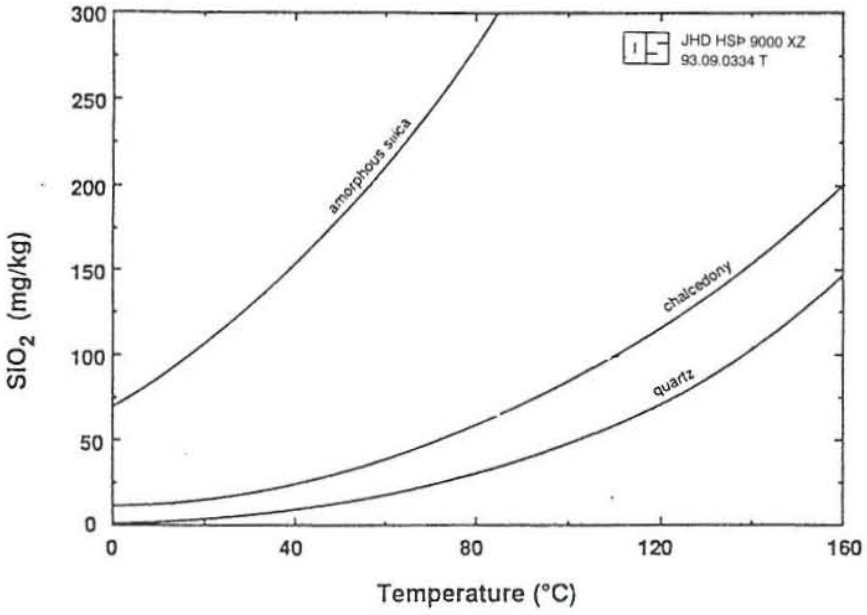

FIGURE 3: Solubility curves of silica minerals with temperature

on the solubilities of quartz and amorphous silica below about 300°C. This information allows the dissolved silica concentration in a hydrothermal solution to be used as a chemical geothermometer. When using the silica geothermometer, an assumption must be made about the particular silica mineral that is controlling the dissolved silica concentration. In other words, the solubilities of different silica minerals are different (Figure 3). Furthermore, below 340°C the solubility of silica decreases drastically as temperature decreases, so silica may polymerize and precipitate from the solution as a result of conductive and/or adiabatic cooling before reaching the surface, causing low estimated reservoir temperatures. As a matter of fact, it is very difficult for silica to precipitate at low reservoir temperatures because the solubility of amorphous silica (i.e. silica species that deposit from geothermal waters), is much greater than those of quartz and chalcedony controlling silica concentrations in high and low temperature reservoirs, respectively.

The silica geothermometers used at present to predict subsurface temperatures of reservoirs are based on experimentally determined solubilities of chalcedony and quartz. Generally speaking, the quartz geothermometer is applied in high temperature reservoirs, but the chalcedony geothermometer in low temperature reservoirs. In Iceland rocks are generally young but the chalcedony geothermometer temperature is used up to 180°C and the quartz geothermometer at higher temperatures. In other countries where rocks may be considerably older quartz equilibrium seems to be obtained at lower temperatures, sometimes down to 90-100°C and in some cases even over the whole temperature range. The reason is that chalcedony is a very fine-grained variety of quartz, composed of aggregates of very tiny crystals. The individual quartz grains are so small that they have relatively large surface energies compared with "normal" quartz, and this results in an increase in solubility. Chalcedony is unstable in contact with water at temperatures above about 120-180°C, because the smallest-sized crystals completely dissolve and larger-sized crystals grow large enough so that surface is no longer a solubility controlling factor. Temperature, time, fluid composition, and prior history all affect the size attained by quartz crystals. Thus, in some places (especially long-lived systems) well-crystallized quartz may control dissolved silica at temperatures less than 100°C, and in others, chalcedony (very fine-grained quartz) may control dissolved silica up to temperatures as high as 180°C (particularly young systems).

Since 1960 many formulae for the estimation of deep temperatures, based on concentrations of silica in thermal waters, have been presented. They result in more or less the same temperatures, but the difference is that the quartz geothermometer yields a higher temperature than the chalcedony geothermometer for the same concentration of silica due to their different equilibration temperatures. Equation 5 for the chalcedony geothermometer, which was presented

by Fournier (1977), and Equation 6 for the quartz geothermometer at the condition of no steam loss by Fournier and Potter (1982) are as follows (the silica concentration, C, is in ppm):

$$t\ (^{\circ}C) = \frac{1023}{(4.69 - \log C)} - 273.15 \tag{5}$$

$$t\ (^{\circ}C) = -\alpha + \beta C - \gamma C^2 + \delta C^3 + \epsilon \log C \tag{6}$$

where

$$\alpha = 42.198;\ \beta = 0.288831;\ \gamma = 3.6686x10^{-4};\ \delta = 3.1665x10^{-7};\ \epsilon = 77.034$$

4.4 Cation geothermometers

4.4.1 The Na-K geothermometer

Cation geothermometry is based on ion exchange reactions with temperature-dependent equilibrium constants. A typical example is the exchange of Na^+ and K^+ between co-existing alkali feldspars:

$$NaAlSi_3O_8 + K^+ = KAlSi_3O_8 + Na^+ \tag{7}$$

If the activities of the solid reactants are assumed to be unity and the activities of the dissolved species are about equal to their molal concentrations, the equilibrium constant, K_{eq}, for Equation 7 is:

$$K_{eq} = \frac{[Na^+]}{[K^+]} \tag{8}$$

For an exchange reaction involving monovalent and divalent ions, such as two K^+ and one Mg^{+2} ions, the equilibrium constant is approximately equal to:

$$K_{eq} = \frac{K^+}{\sqrt{Mg^{+2}}} \tag{9}$$

The equilibrium constant changes with temperature, so it is possible to calculate subsurface temperatures based on the concentrations of the ions in hot waters. Experiments at high temperature and pressure by Orville (1963) and Hemley (1967) showed, however, that reactions involving base exchange of Na and K between alkali feldspars and an aqueous solution, proceed very slowly at temperature below about 300°C. In addition, the Na-K exchange reaction generally takes longer than the silica dissolution reaction to reach water-rock equilibrium. Therefore there is a tendency to use the Na/K ratio to estimate possible high temperatures in the deeper parts of a system where waters reside for relatively long periods. Other geothermometers are applied to evaluate relatively low temperatures which are observed in shallow reservoirs where waters stay for relatively short periods.

Many temperature functions have been presented for the Na-K geothermometer, but there is a large discrepancy between the different equations at low temperature. Equations 10, 11 and 12

presented by Giggenbach (1988), Arnorsson et al. (1983b) and Fournier (1979), respectively have been utilized to predict subsurface temperatures in the Guanzhong basin (concentrations of Na, K and Mg in ppm):

$$t(^\circ C) = \frac{1390}{1.75 + \log\frac{Na}{K}} - 273.15 \tag{10}$$

$$t(^\circ C) = \frac{933}{0.780 + \log\frac{Na}{K}} - 273.15 \tag{11}$$

$$t(^\circ C) = \frac{1217}{1.483 + \log\frac{Na}{K}} - 273.15 \tag{12}$$

The temperature functions proposed by Arnorsson et al. (1983b) and Fournier (1979) are based on borehole data. It is considered that Giggenbach's temperature function tends to give too high results even though there is some experimental evidence.

4.4.2 Na-K-Ca geothermometer

The Na-K-Ca geothermometer (Fournier and Truesdell, 1973) takes into account reactions involving the exchange of Na^+, K^+ and Ca^{+2} with mineral solid solutions. The geothermometer is completely empirical and assumes one type of base exchange reaction at temperatures above about 100°C:

$$K^+ + Na_{\frac{2}{3}}Ca_{\frac{1}{6}}\text{-}solid = \frac{1}{6}Ca^{+2} + \frac{2}{3}Na^+ + K\text{-}solid \tag{13}$$

and a different exchange reaction at temperature below about 100°C:

$$K^+ + \frac{1}{3}Na^+ + Ca_{\frac{2}{3}}\text{-}solid = \frac{2}{3}Ca^{+2} + KNa_{\frac{1}{3}}\text{-}solid \tag{14}$$

Using Equations 13 and 14, Fournier and Truesdell, (1973) presented the following equation (the concentrations of Na^+, K^+, and Ca^{+2} in ppm):

$$t(^\circ C) = \frac{1647}{\log\frac{Na}{K} + \beta\left(\log\frac{\sqrt{Ca}}{Na} + 2.06\right) + 2.47} - 273.15 \tag{15}$$

where

$$\beta = \frac{4}{3} \text{ for } t < 100\ ^\circ C; \quad \beta = \frac{1}{3} \text{ for } t > 100\ ^\circ C$$

Furthermore, Fournier and Potter (1979) presented a magnesium correction to this geothermometer.

4.4.3 K-Mg geothermometer

Giggenbach et al. (1983) presented the following geothermometer, which was later slightly revised by Giggenbach, (1988).

$$t(^{\circ}C) = \frac{4410}{14.0 - \log\frac{K}{\sqrt{Mg}}} - 273.15 \qquad (16)$$

The geothermometer is utilized for hot waters form Guanzhong basin to obtain subsurface temperatures which are slightly lower than the other geothermometer temperatures.

4.5 Application of silica and cation geothermometers

Eleven water samples from the Guanzhong basin have been used to predict possible subsurface temperatures by means of silica and cation geothermometers (Table 3). The measured temperatures are in the range 43-72°C. All the calculated geothermometer temperatures seem to be reasonable, except the Na-K geothermometer temperatures, but there is temperature difference of 20-40°C between different geothermometer temperatures. Generally, the Na-K-Ca and quartz geothermometers yield more or less the same temperatures, which are higher than the chalcedony and K-Mg geothermometer temperatures. All the Na-K geothermometers give too high values for the first four samples (S1, W2, S3 and S8) but Fournier's (1979) geothermometer apparently agrees with some others. In the Guanzhong basin the thermal waters originally come from the old metamorphic formations, and they may reach the deep reservoir because of the faults and fissures as a result of repeated tectonic activity, so it seems possible that quartz dissolution and base exchange reactions involving quartz, clays and mica are a major controlling factor. The low K-Mg geothermometer temperatures, similar to the measured temperatures, probably result from the re-equilibrium of hot waters.

TABLE 3: Chemical geothermometer temperatures for thermal waters from the Guanzhong basin, China

No.	$T_{mea.}$	$T_{qtz.}$	$T_{cha.}$	T_{NaK1}	T_{NaK2}	T_{NaK3}	T_{KMg}	T_{NaKCa}
S1	60.0	119.6	90.9	186.4	136.1	166.3	/	126.7
W2	58.0	107.8	78.0	185.1	135.9	166.0	92.8	125.6
S3	43.0	89.8	58.5	175.5	125.4	156.7	57.1	94.7
S8	58.0	105.0	75.1	183.3	137.0	167.0	59.9	106.8
W7	61.0	77.4	45.1	70.0	10.0	48.5	50.2	96.9
W9	62.0	102.1	71.7	95.1	38.0	75.7	58.2	84.1
W12	65.0	86.6	55.1	73.7	13.4	51.7	49.2	88.4
W4	63.9	102.2	71.9	/	/	/	/	/
W5	47.0	70.8	38.7	/	/	/	/	/
W10	52.0	79.2	47.3	/	/	/	/	/
W11	72.0	74.06	42.0	/	/	/	/	/

T_{NaK1}, T_{NaK2} and T_{NaK3} are based on Giggenbach (1988), Arnorsson et al. (1983b) and Fournier (1979).

5. EQUILIBRIUM STATE OF THE GEOTHERMAL WATERS

There tend to be equilibrium relationships between aqueous solutions and minerals in geothermal reservoirs, especially in high-temperature systems, on the basis of which subsurface temperatures can be predicted. However, in some cases, the components that are potential geoindicators are not really in equilibrium with the appropriate minerals due to low temperatures in the reservoirs, mixing with cold water or possible chemical reactions. Therefore, it is very important to study the equilibrium state of thermal waters to check the reliability of geothermometers. As a matter of fact, different subsurface temperatures are sometimes obtained for the same sample. The most reliable temperature must be confirmed by a further study. First, a log(Q/K) diagram is used to reveal possible subsurface temperatures as derived from potential equilibria for all minerals that are likely to participate. Then, standard curves for different chemical compositions at the reference temperatures are prepared to reveal which type of silica geothermometer is appropriate for specified condition. Finally, the Na-K-Mg triangular diagram is applied to evaluate the equilibrium state of water samples.

5.1 The log(Q/K) diagram for S3

Using the results of the aqueous speciation calculations the degree of saturation of minerals in aqueous solutions at different temperatures, the saturation index, SI, can be estimated:

$$SI = \log \frac{Q}{K} = logQ - logK \qquad (17)$$

where Q is the calculated ion activity product and K is the equilibrium constant. Therefore, the SI value for each mineral gives an estimate of the equilibrium state. Values of SI more than, equal to and less than zero represent respectively supersaturation, equilibrium and undersaturation.

The WATCH programme is very convenient for the calculation of Q and K at different temperatures on the basis of the calculated chemical speciation in natural waters (Appendix I). After that, a log(Q/K) vs. temperature diagram can be drawn to show SI (Figure 4). If a mineral is in equilibrium with the aqueous solution, the temperature corresponding to the intersection point of the mineral equilibrium curve and the SI = 0 line is its theoretical equilibrium temperature. This characteristic of convergence of log(Q/K) curves for the mineral assemblage to zero at the temperature of equilibrium can be used to confirm the most probable geothermometer temperature at which the mineral used as a chemical thermometer reaches or approaches the equilibrium line (SI = 0) (Reed and Spycher, 1984). D'Amore et al., (1987) have used this approach for the interpretation of geothermal spring chemistry, and Tole et al., (1993) have tested its validity on data from boreholes, both with success.

The analytical data from the Lintong hot spring are used to calculate the equilibrium state for 23 minerals. Only 19 curves have been drawn so as to make the diagram clear (Figure 4). It shows that 6 curves converge in the range of 55-65°C, where chalcedony equilibrates with the hot water at about 60°C, and it is thus inferred that chalcedony rather than quartz probably controls the fluid-silica equilibrium in the geothermal system. In other words, the chalcedony geothermometer temperature is more reliable than subsurface temperatures predicted by quartz geothermometer in the area. Calcium carbonate equilibrium temperature is similar to the sampling temperature, 42.5°C, while the fluorite equilibrium temperature is higher than the equilibrium temperature of the system. The use of log(Q/K) diagrams to obtain equilibrium temperatures is a little subjective being based on an individual's impression of possible or real equilibria between fluid and mineral assemblage. Furthermore, statistical methods can be used to determine the temperature ranges where the saturation indices of most minerals cross the horizontal line.

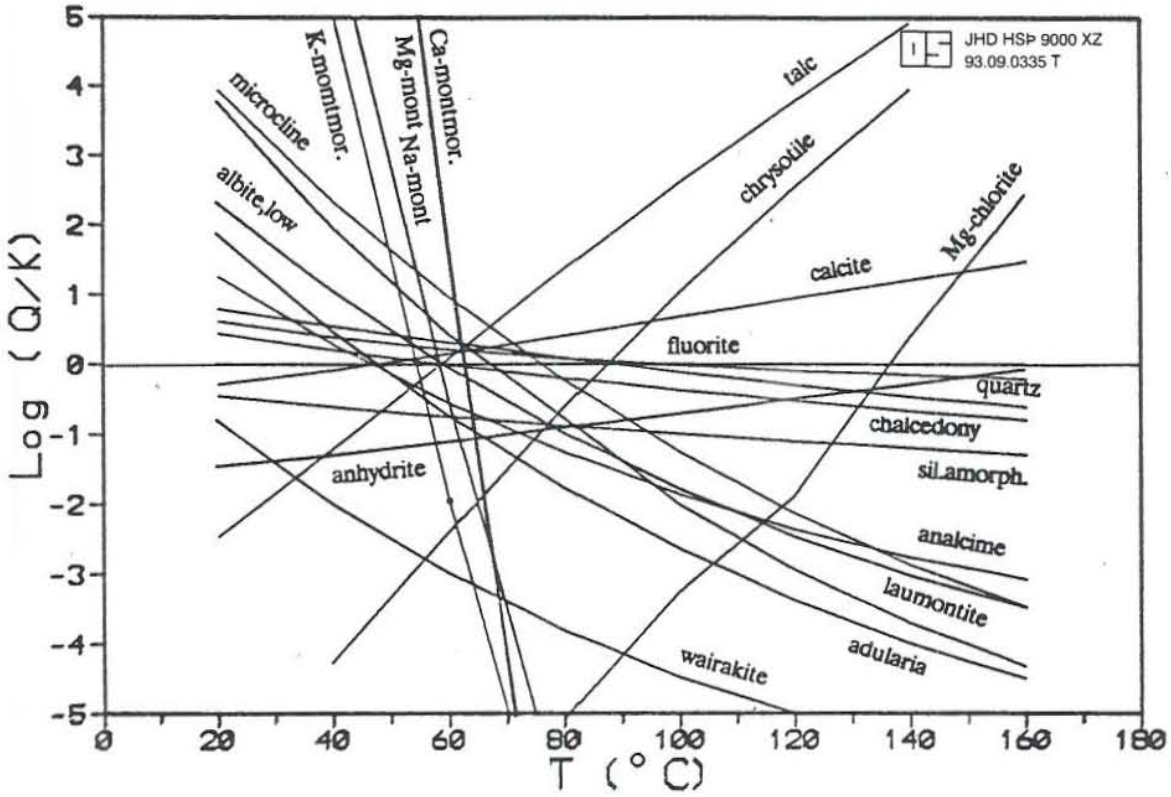

FIGURE 4: Mineral equilibrium curves for waters from S3 in Lintong, China

5.2 Equilibrium state at reference temperatures

The chemical analytical data for the water S3 have been used to predict probable subsurface temperatures from the log(Q/K) diagram. Unfortunately, the S3 chemical data are the only ones from Guanzhong basin that include aluminium and iron concentrations. The diagram describing the temperature dependence of cation/proton ratios at different reference temperatures are drawn to estimate the equilibrium state between waters and minerals, and can be applied to further reveal the water-mineral equilibrium state. The equations are applied to describe the temperature dependence of cation/proton ratios and undissociated weak acid concentrations in ppm as follows (Arnorsson et al., 1983a):

$$\log H_4SiO_4^\circ = -0.588 - 0.00441T - \frac{1515.21}{T} + 1.347 \log T \tag{18}$$

$$\log H_2CO_3^\circ = -1.794 - 0.0051T - \frac{4469.63}{T} + 4.1414 \log T \tag{19}$$

$$\log H_2S^\circ = -1.678 - 0.00355T - \frac{5071.05}{T} + 3.8889 \log T \tag{20}$$

$$\log H_2SO_4^\circ = -6.436 - 0.03906T - \frac{13335.68}{T} + 14.7958 \log T \tag{21}$$

$$logHF^{\circ} = -5.262 - 0.03511T - \frac{7964.11}{T} + 12.1022logT \quad (22)$$

$$\log\frac{Na^{+}}{H^{+}} = 2.694 + 0.02023T + \frac{4243.47}{T} - 6.2069logT \quad (23)$$

$$\log\frac{K^{+}}{H^{+}} = 2.505 + 0.01971T + \frac{3325.71}{T} - 5.7814logT \quad (24)$$

Generally, it is impossible for all chemical reactions to reach water-rock equilibrium, but we can evaluate the equilibrium state of a water sample from the relation between the equilibrium concentrations and the calculated concentrations at different temperatures in deep reservoirs (Figures 5 and 6). It seems that all the points are closer to equilibrium curves, except the log Q calcite and log H_4SiO_4 vs. temperature, at the quartz temperatures (Figure 6), than at the chalcedony temperatures (Figure 5), but most of the points are still off the equilibrium curves at the quartz temperatures. By comparing Figure 5 with Figure 6, samples S1, W2 and S8 from the foot of Qinling mountain, obviously approach the equilibration lines, more closely at the quartz than at the chalcedony temperature. This may show that quartz controls the concentrations of silica in the deep reservoir, or at least that quartz is a better geothermometer for the evaluation of the subsurface temperatures at depth in the Guanzhong basin.

5.3 The Na-K-Mg triangular diagram

Cation geothermometry, based on Na-K, Na-K-Ca and K-Mg equilibrium states, is a useful tool for the evaluation of the subsurface temperatures in the Guanzhong basin. Most of the problems in their use arise from their application to unsuitable samples. The use of pH or their relative Cl^{-}, SO_4^{-2} and HCO_3^{-} concentrations to exclude unsuitable samples go a long way to improve their reliability. Recently a "self-policing" technique was presented to give an automatic indication as to the suitability of a given chemical analytical result for the application of ionic solute geothermometers. It is essentially based on the temperature dependence of the two reactions:

$$K\text{-}feldspar + Na^{+} = Na\text{-}feldspar + K^{+} \quad (25)$$

and

$$92.8K\text{-}feld. + 1.6H_2O + Mg^{+2} = 0.8K\text{-}mica + 0.2Chlo. + 5.4Sil. + 2K^{+} \quad (26)$$

where feld., Chlo. and Sil. refer to feldspar, chloride and silica, respectively. Both involve minerals of the full equilibrium assemblage expected to be produced after the isochemical recrystallization of an average crustal rock under conditions of geothermal interest. Na^{+}, K^{+} and Mg^{+2} concentrations of waters in equilibrium with this assemblage are accessible to rigorous evaluation. The theoretical temperature dependence of the corresponding concentration quotients may then be applied to derive the two geothermometers, defined as Equations 10 and 16.

When applied to waters in the Guanzhong basin, individual utilization of Equations 10 and 16 often leads to significantly different temperatures of equilibrium. For instance, the temperatures obtained by the K-Mg geoindicator are generally lower than those obtained by other geothermometers and are close to the measured temperatures. This observation can be explained in terms of different re-adjustment rates of the two reactions to changes in the physical

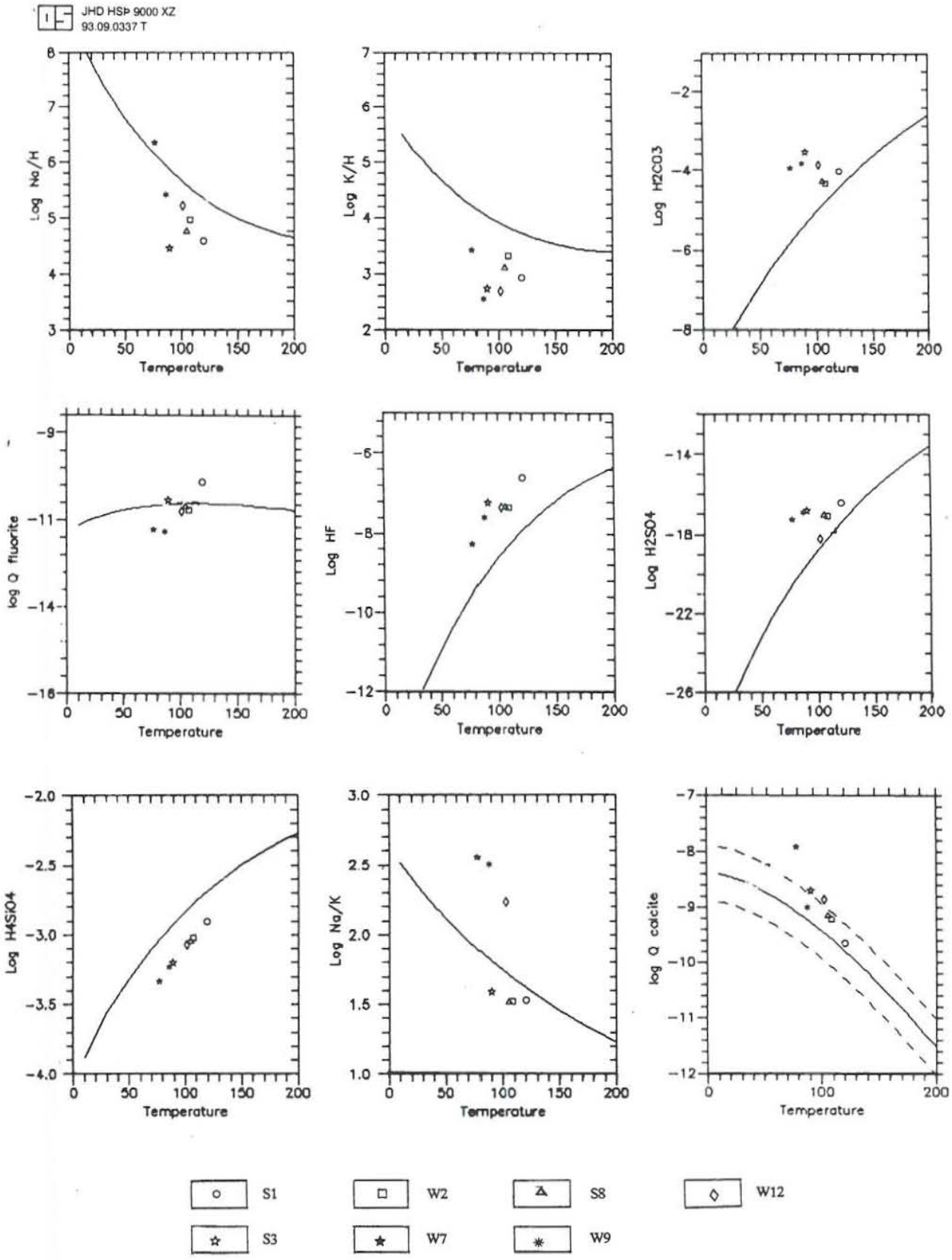

FIGURE 5: Equilibrium state for hot waters from the Guanzhong basin at the chalcedony geothermometer temperatures

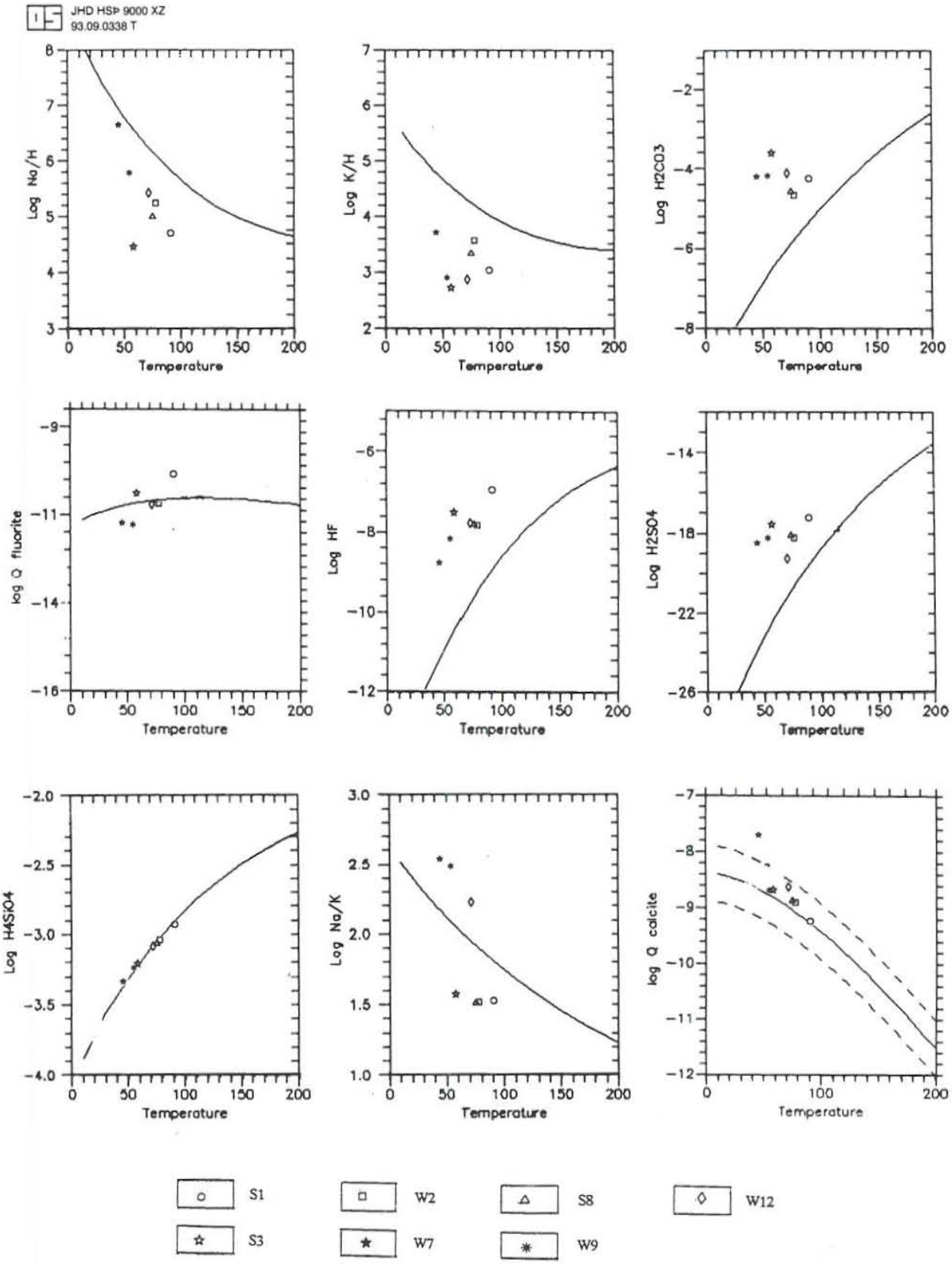

FIGURE 6: Equilibrium state for hot waters from the Guanzhong basin at the quartz geothermometer temperatures

environment encountered by the up-flow waters. Equation 16 was found to respond much faster and, therefore, usually give lower temperature estimates. It is also very sensitive to the admixture of non-equilibrium acid waters, while Equation 10 is much less affected by such shallow processes. By combining the two sub-systems, a method for evaluating the degree of water-rock equilibrium and eliminating unsuitable samples is obtained.

The triangular diagram of Giggenbach (1988) has been used for Guanzhong basin waters. The coordinates for Figure 7 are calculated as follows:

$$S = \frac{Na^+}{1000} + \frac{K^+}{100} + \sqrt{Mg^{+2}} \tag{27}$$

$$Na\% = \frac{Na^+}{10S} \tag{28}$$

$$Mg\% = \frac{100\sqrt{Mg^{+2}}}{S} \tag{29}$$

Samples W7, W9 and W12 from deep geothermal wells in the inner basin plot on the full equilibrium line, so the Na-K geothermometer presented by Giggenbach (1988) will be applied to estimate the subsurface temperatures for these samples. W2 and S8 plot in the partial equilibrium area, and S3 in the area of immature waters which may arise from admixture with shallow cold waters. Although W2 departs somewhat from the equilibrium line, its position on the diagram probably infers a potentially high temperature in the deep reservoir (Figure 7).

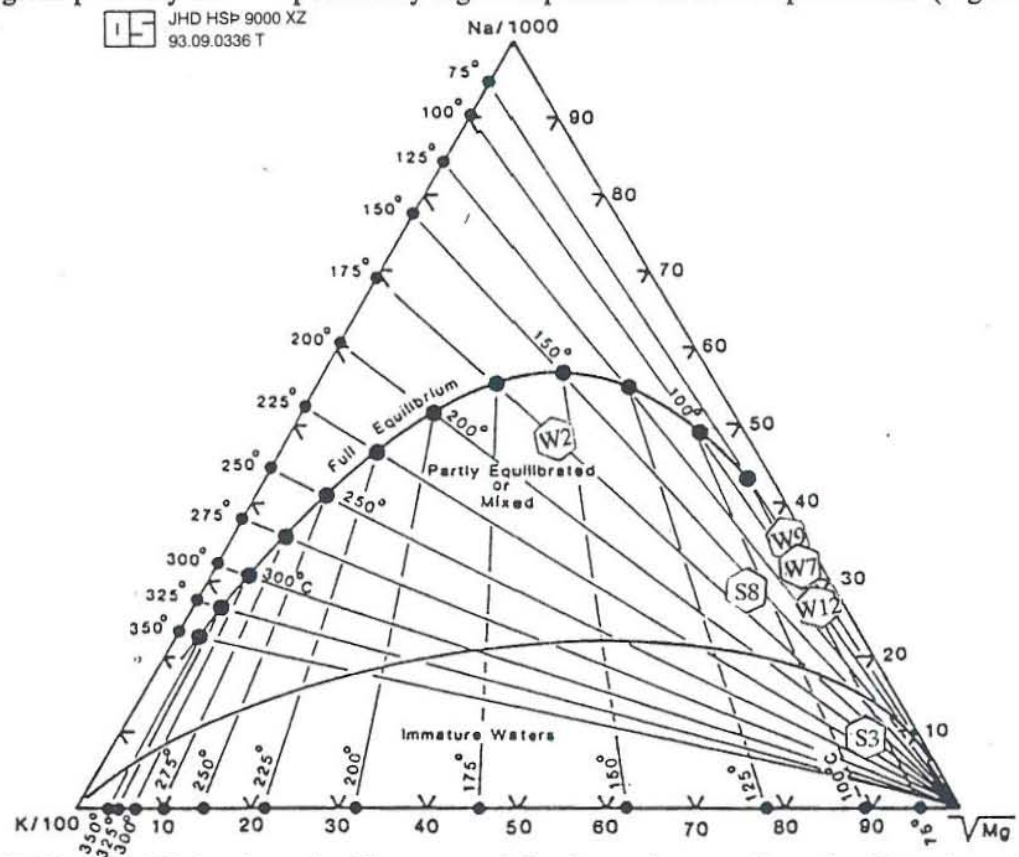

FIGURE 7: Na-K-Mg triangular diagram used for thermal waters from the Guanzhong basin

6. ESTIMATES OF SUBSURFACE TEMPERATURES

As shown before, many geothermometers have been used to predict subsurface temperatures, and may give different temperatures for the same sample. The study of mineral equilibrium states is utilized to check the results of chemical geothermometers, that is to say, if a mineral does not equilibrate with hot water in geothermal systems, the predicted temperatures from the geothermometers are not reliable.

6.1 Hot waters along the border of Qinling and the basin

The hot wells and hot springs lie on the border line of Qinling mountains and the basin (Figure 2). Their chemical composition and the geothermometer temperatures of their waters are listed in Tables 2 and 3 separately. There are four samples available, one from spring S1 in Meixian, one from spring S8, one from well W2 in Lantian, and one from spring S3 in Lintong.

For S1, W2 and S8, the quartz temperatures (105-119.6°C) are close to the Na-K-Ca temperatures (106-126.7°C). The calculated chalcedony temperatures (75.1-90.9°C) are lower than the quartz and Na-K-Ca temperatures. The equilibrium studies (Figures 5 and 6) show that the S1, W2 and S8 waters match equilibrium curves at the quartz reference temperatures much better than at the chalcedony temperature except for the log H_4SiO_4 and log $Q_{calcite}$ curves. It seems possible that quartz rather than chalcedony controls silica concentrations at the foot of Qinling mountain. In other words, there may be geothermal water with subsurface temperatures of 100-120°C along the Qinling fault zone.

Sample S3 is from a hot spring at the foot of Li mountain, a part of Qinling mountain. The good convergence temperature (about 60°C), with 6 minerals equilibrating in a temperature range of 10°C, obtained from the log (Q/K) diagram indicates that the hot water is in equilibrium with chalcedony (Figure 4). On the other hand, the fact that the S3 water plots in the area of immature waters on the Na-K-Mg triangular diagram (Figure 7), shows that most of the hot water derives from shallow cold water so, the chemical geothermometers cannot be used for this water sample. However, the temperature of 60°C possibly represents the minimum deep temperature in the area, because the Na-K and Na-K-Ca temperatures, which are less sensitive to mixing with cold water than silica temperatures, are higher than the silica temperatures.

6.2 Hot waters in the inner basin

All the samples from the inner basin are from boreholes, most of which are located in an area not far from Qinling mountain.

Samples W7, W9 and W12 were collected from 1700 m or deeper boreholes, whose aquifers are in Tertiary clastic rock. The Na-K temperatures (70-95.6°C) (Giggenbach, 1988) and Na-K-Ca temperatures (84-96.9°C) are similar to the quartz temperatures (77.4-102.1°C), but higher than chalcedony temperatures (45.1-71.9°C) and K-Mg temperatures (49.2-58.2°C), which are even slightly lower than the measured temperatures (58-65°C). As a result, the K-Mg and chalcedony chemical geothermometers are considered unreliable. Furthermore, in this case the three waters plot on the full equilibrium line on the Na-K-Mg triangular diagram (Figure 7) so the Na-K temperatures (Giggenbach, 1988) listed in Table 3 are probable subsurface temperatures for samples W7, W9, and W12.

Sample W4 was collected from a 2000 m deep borehole about 400 m away from well W12. Its aquifer is also in Tertiary clastic rock. The chalcedony temperature (71.9°C) is the same as the measured temperature (71.2°C) at the bottom of the hole, being lower than the quartz temperature (102.2°C). It is difficult to decide whether chalcedony or quartz controls the concentration of silica, because the sample has only been analyzed for combined Na and K, but not for Al and Fe.

For samples W5, W10 and W11, the quartz geothermometer yields temperatures (70.8-79.2°C) higher than the chalcedony temperatures (38.7-47.2°C). The latter are lower than the measured temperatures (52-72°C). However, there are no other geothermometer temperatures available for the same reasons as for W4, and so the temperature of 70-80°C is considered to be their probable subsurface temperature.

7. CONCLUSIONS AND RECOMMENDATIONS

The geotectonic conditions play an important role in controlling geothermal activity and the distribution of thermal water. The tectonic channels, like faults and fissures, provide the flow paths and the storage space for hot water, and different mineral compositions affect the components of thermal waters. In the Guanzhong basin, thermally anomalous areas are controlled by different faults, mainly the Qinling deep, long fault along which many hot springs issue. Temperature and chemical composition of thermal waters from boreholes and springs in the basin suggest that their sources or at least their discharge channels may be different. Although all the hot waters obtained are below boiling point, the chemical equilibrium studies show that the hot waters from the thermal springs and wells may reach or approach equilibrium with quartz, because the water possibly circulates slowly and reaches the deep crust.

A reliable method for the collection of samples from thermal manifestations is of great importance for obtaining good geochemical data. The chemical speciation calculations with the programme WATCH show a good anion-cation balance for the chemical data on hot waters from Guanzhong basin. This lays a solid foundation for the use of geothermometry and chemical equilibrium calculations.

One important assumption for the use of geothermometers is that the thermal water is in equilibrium with minerals in the deep reservoir. Actually most of the hot water samples depart, to some extent, from the equilibrium state because of the low temperature in the deep systems, or physical processes like mixing with cold water and/or degassing on the surface. If so, the studies of water-rock equilibrium state become very important for deciding whether a specified water sample can be used to predict the possible subsurface temperature. It is suggested that several geothermometers should be used at the same time, and then the geothermometer temperatures should be verified or eliminated by the evaluation of their water-rock equilibrium states.

The major geothermometers have been used for predicting the subsurface temperatures in the Guanzhong basin. Most of the geothermometer temperatures are reasonable, with a temperature variation of 20-30°C. The co-application of geothermometers and the methods for studying water-rock equilibrium show that there may be maximum temperatures of 100-120°C in the deep reservoirs along the Qinling fault, but in the inner basin the subsurface temperatures are probably lower than 100°C. The zone at the foot of Qinling mountain is a promising area for a geothermal development with regard to economy and exploitation potential.

As mentioned above, reliable chemical analytical data are very important for the application of geothermometry, but there are not enough analytical data on these thermal waters available. In addition, almost all the chemical data do not include the Fe and Al concentrations, and in some samples only the combined concentrations of Na and K have been determined, making it difficult to use the programme WATCH to carry out the equilibrium calculations. At the same time, some useful elements like Li, B, Br, I, etc. should be analyzed to give valuable information on the geothermal reservoirs studied. If the data are improved, more reliable results will be obtained.

ACKNOWLEDGEMENTS

I wish to express my gratitude to my advisor Dr. Halldor Armannsson and Mr. Jon Orn Bjarnason for their excellent guidance and evaluation of the report.

Special thanks are due to Dr. Ingvar Birgir Fridleifsson, the director of the UNU Geothermal Training Programme for offering me the opportunity to attend the course and for providing excellent work conditions during my entire study.

I also would like to thank Mr. Ludvik S. Georgsson and Ms. Margret Westlund for their help in various ways, and carefully editing the report. My thanks also go to the ladies in the drawing office for completing some of my figures in this report.

I am very grateful to all the lecturers for their comprehensive presentations, specially to the staff of the Chemical Division and Dr. Stefan Arnorsson at the University of Iceland for their willingness to share their knowledge and their experience.

Finally, the author is grateful to professor Hongjun Liu for his help in providing all the data used in the report, and to Xi'an College of Geology for giving me the opportunity to participate the training programme.

REFERENCES

Arnorsson, S., and Bjarnason, J.O., 1993: Icelandic Water Chemistry Group presents the chemical speciation programme WATCH. Science Institute, University of Iceland, Orkustofnun, Reykjavik, 7 pp.

Arnorsson, S., and Gunnlaugsson, E., 1985: New gas geothermometers for geothermal exploration - calibration and application. Geochim. Cosmochim. Acta, 49, 1307-1325.

Arnorsson, S., Sigurdsson, S., and Svavarsson, H., 1982: The chemistry of geothermal waters in Iceland. I. Calculation of aqueous speciation from 0° to 370°C. Geochim. Cosmochim. Acta, 46, 1513-1532.

Arnorsson, S., Gunnlaugsson, E., and Svavarsson, H., 1983a: The chemistry of geothermal waters in Iceland. II. Mineral equilibria and independent variables controlling water compositions. Geochim. Cosmochim. Acta, 47, 547-566.

Arnorsson, S., Gunnlaugsson, E., and Svavarsson H., 1983b: The chemistry of geothermal waters in Iceland. III. Chemical geothermometry in geothermal investigations. Geochim. Cosmochim. Acta, 47, 567-577.

Bodvarsson, G., and Palmason, G., 1961: Exploration of subsurface temperatures in Iceland. U.N. Conference on New Sources of Energy, Rome, G/24., Jokull, 11, 39-48.

D'Amore, F., Fancelli, R., and Caboi, R., 1987: Observation on the application of chemical geothermometers to some hydrothermal systems in Sardinia. Geothermics, 16, 271-282.

D'Amore, F., and Panichi, C., 1980: Evaluation of deep temperatures in hydrothermal systems by a new gas geothermometer. Geochim. Cosmochim. Acta, 44, 549-556.

Darling, W.G., and Talbot, J.C., 1992: Hydrocarbon gas ratio geothermometry in the East African Rift System. In: Kharaka, Y.K. and Maest, A.S. (editors), Water-Rock Interaction. Balkema, Rotterdam, 1441-1444.

Ellis, A.J., and Wilson, S.H., 1960: The geochemistry of alkali metal ions in the Wairakei hydrothermal system. New Zealand J. Geol. Geophys., 3, 593-617.

Fouillac, C., and Michard, G., 1981: Sodium/lithium ratio in water applied to geothermometry of geothermal reservoirs. Geothermics, 10, 55-70.

Fournier, R.O., 1977: Chemical geothermometers and mixing models for geothermal systems. Geothermics, 5, 41-50.

Fournier, R.O., 1979: A revised equation for the Na/K geothermometer. Geothermal Resources Council, Transactions, 3, 221-224.

Fournier, R.O., and Potter, R.W. II., 1979: Magnesium correction to the Na-K-Ca chemical geothermometer. Geochim. Cosmochim. Acta, 43, 1543-1550.

Fournier, R.O., and Potter, R.W. II., 1982: A revised and expanded silica [quartz] geothermometer. Geothermal Resources Council, Bulletin, 3-12.

Fournier, R.O., and Rowe, J.J., 1966: Estimation of underground temperatures from the silica content of water from hot springs and wet steam wells. Am. J. Sci., 264, 685-697.

Fournier, R.O., and Truesdell, A., 1973: An empirical Na-K-Ca geothermometer for natural waters. Geochim. Cosmochim. Acta, 37, 1255-1275.

Giggenbach, W.F., 1988: Geothermal solute equilibria. Derivation of Na-K-Mg-Ca geoindicators. Geochim. Cosmochim. Acta, 52, 2749-2765.

Giggenbach, W.F., Gonfiantini, R., Jangi, B.L., and Truesdell, A.H., 1983: Isotopic and chemical composition of Parbati Valley geothermal discharges, NW-Himalaya, India. Geothermics, 12, 199-222.

Hemley, J.J., 1967: Aqueous Na/K ratios in the system K_2O-Na_2O-Al_2O_3-SiO_2-H_2O. Program, 1967 Ann. Meeting Geol. Soc. Amer., New Orleans, 94-95.

Liu, L.H., 1975: Investigation of geothermal resources in the Guanzhong basin. Shaanxi Geological Bureau, report, 130 pp.

Olafsson, M., 1988: Sampling methods for geothermal fluids and gases. Orkustofnun, Reykjavik, report OS-88041/JHD-06, 17 pp.

Orville, P.M., 1963: Alkali ion exchange between vapour and feldspar phases. Amer, J. Sci., 261, 201-237.

Reed, M., and Spycher, 1984: Calculation of pH and mineral equilibria in hydrothermal waters with application to geothermometry and studies of boiling and dilution, Geochim. Cosmochim. Acta, 48, 1479-1490.

Tole, M.P., Armannsson, H., Pang Zhong-he, and Arnorsson, S., 1993: Fluid/mineral equilibrium calculations for geothermal fluids and chemical geothermometry. Geothermics, 22, 17-37.

APPENDIX I: Printouts from the programme WATCH

OREKUSTOFNUN LINTONG.CHAL

==========

S3 LINTONG

Program WATCH

Water sample (mg/kg)		Steam sample					
pH/deg.C	7.50/ 12.0	Gas (volume %)		Reference temperature	deg.C :	58.5	(Chalcedony)
CO2	152.20	CO2	.00				
H2S	.00	H2S	.00	Sampling pressure	bar abs. :	1.0	
NH3	.01	NH3	.00	Discharge enthalpy	kJ/kg :	245.	(Calculated)
B	.00	H2	.00	Discharge	kg/s :	4.0	
SiO2	38.30	O2	.00	Steam fraction at collection	:	.0000	
Na	187.30	CH4	.00				
K	8.40	N2	.00	Measured temperature	deg.C :	43.0	
Mg	3.600						
Ca	40.10	Liters gas per kg					
F	5.620	condensate/deg.C	.00/ .0	Condensate (mg/kg)			
Cl	128.70			pH/deg.C	.00/ .0		
SO4	217.60	Total steam (mg/kg)		CO2	.00		
Al	.010	CO2	.00	H2S	.00		
Fe	.010	H2S	.00	NH3	.00		
TDS	782.00	NH3	.00	Na	.00		

Ionic strength = .01416
Ionic balance : Cations (mol.eq.) .01044699 Anions (mol.eq.) .01145118 Difference (%) -9.17

Deep water components (mg/kg)				Deep steam (mg/kg)		Gas pressures (bars-abs.)	
B	.00	CO2	152.20	CO2	.00	CO2	.154E-01
SiO2	38.30	H2S	.00	H2S	.00	H2S	.000E+00
Na	187.30	NH3	.01	NH3	.00	NH3	.411E-08
K	8.40	H2	.00	H2	.00	H2	.000E+00
Mg	3.600	O2	.00	O2	.00	O2	.000E+00
Ca	40.10	CH4	.00	CH4	.00	CH4	.000E+00
F	5.620	N2	.00	N2	.00	N2	.000E+00
Cl	128.70					H2O	.186E+00
SO4	217.60					Total	.201E+00
Al	.0100						
Fe	.0100						
TDS	782.00	Aquifer steam fraction =	.0000				

Ionic strength = .01382 1000/T (Kelvin) = 3.02
Ionic balance : Cations (mol.eq.) .01027247 Anions (mol.eq.) .01127755 Difference (%) -9.33

Chemical geothermometers (degrees C)

Quartz	89.8	(Fournier & Potter, GRC Bulletin, pp. 3-12, Nov. 1982)
Chalcedony	58.5	(Fournier, Geothermics, vol. 5, pp. 41-50, 1977)
Na/K	124.8	(Arnorsson et al., Geochim. Cosmochim. Acta, vol. 47, pp. 567-577, 1983)

Oxidation potential (volts) : Eh H2S= 99.999 Eh CH4= 99.999 Eh H2= 99.999 Eh NH3= 99.999

Activity coefficients in deep water

H+	.897	KSO4-	.886	Fe++	.623	FeCl+	.881
OH-	.879	F-	.879	Fe+++	.379	Al+++	.379
H3SiO4-	.881	Cl-	.877	FeOH+	.884	AlOH++	.618
H2SiO4--	.618	Na+	.881	Fe(OH)3-	.884	Al(OH)2+	.886
H2BO3-	.875	K+	.877	Fe(OH)4--	.614	Al(OH)4-	.882
HCO3-	.881	Ca++	.623	Fe(OH)++	.614	AlSO4+	.882
CO3--	.609	Mg++	.641	Fe(OH)2+	.886	Al(SO4)2-	.882
HS-	.879	CaHCO3+	.888	Fe(OH)4-	.886	AlF++	.618
S--	.614	MgHCO3+	.881	FeSO4+	.884	AlF2+	.886
HSO4-	.882	CaOH+	.888	FeCl++	.614	AlF4-	.882
SO4--	.604	MgOH+	.889	FeCl2+	.884	AlF5--	.609
NaSO4-	.886	NH4+	.875	FeCl4-	.881	AlF6---	.328

Chemical species in deep water - ppm and log mole

Deep water pH is 7.320

H+	.00	-7.273	Mg++	2.58	-3.974	Fe(OH)3	.00	.000
OH-	.04	-5.682	NaCl	.10	-5.786	Fe(OH)4-	.00	.000
H4SiO4	60.61	-3.200	KCl	.00	-7.555	FeCl+	.00	-9.314
H3SiO4-	.60	-5.199	NaSO4-	3.12	-4.581	FeCl2	.00	-25.851
H2SiO4--	.00	-8.999	KSO4-	.40	-5.527	FeCl++	.00	.000
NaH3SiO4	.06	-6.289	CaSO4	14.79	-3.964	FeCl2+	.00	.000
H3BO3	.00	.000	MgSO4	4.62	-4.416	FeCl3	.00	.000
H2BO3-	.00	.000	CaCO3	.66	-5.182	FeCl4-	.00	.000
H2CO3	16.92	-3.564	MgCO3	.03	-6.393	FeSO4	.00	-7.669
HCO3-	190.62	-2.505	CaHCO3+	4.54	-4.348	FeSO4+	.00	.000
CO3--	.40	-5.180	MgHCO3+	.27	-5.497	Al+++	.00	-15.490
H2S	.00	.000	CaOH+	.00	-7.596	AlOH++	.00	-12.016
HS-	.00	.000	MgOH+	.00	-7.469	Al(OH)2+	.00	-9.002
S--	.00	.000	NH4OH	.00	-7.307	Al(OH)3	.01	-6.986
H2SO4	.00	-17.562	NH4+	.01	-6.269	Al(OH)4-	.05	-6.575
HSO4-	.00	-7.744	Fe++	.01	-6.831	AlSO4+	.00	-15.532
SO4--	200.67	-2.680	Fe+++	.00	.000	Al(SO4)2-	.00	-16.464
HF	.00	-7.448	FeOH+	.00	-8.025	AlF++	.00	-12.170
F-	5.62	-3.529	Fe(OH)2	.00	-10.890	AlF2+	.00	-10.177
Cl-	128.64	-2.440	Fe(OH)3-	.00	-15.314	AlF3	.00	-9.712
Na+	186.65	-2.091	Fe(OH)4--	.00	-21.392	AlF4-	.00	-10.839
K+	8.28	-3.674	Fe(OH)++	.00	.000	AlF5--	.00	-12.929
Ca++	33.68	-3.075	Fe(OH)2+	.00	.000	AlF6---	.00	-15.863

Log solubility products of minerals in deep water

	Theor.	Calc.		Theor.	Calc.		Theor.	Calc.
Adularia	-19.174	-19.817	Albite, low	-18.268	-18.232	Analcime	-14.543	-15.032
Anhydrite	-5.065	-6.180	Calcite	-8.820	-8.676	Chalcedony	-3.210	-3.200
Mg-Chlorite	-82.258	-89.311	Fluorite	-10.681	-10.451	Goethite	-6.140	99.999
Laumontite	-29.595	-29.053	Microcline	-20.879	-19.817	Magnetite	-32.879	99.999
Ca-Montmor.	-98.179	-95.630	K-Montmor.	-48.458	-49.906	Mg-Montmor.	-99.088	-96.516
Na-Montmor.	-48.305	-48.320	Muscovite	-24.223	-21.313	Prehnite	-38.721	-40.609
Pyrrhotite	-120.665	99.999	Pyrite	-178.648	99.999	Quartz	-3.534	-3.200
Wairakite	-26.143	-29.053	Wollastonite	12.261	8.160	Zoisite	-37.459	-41.356
Epidote	-47.004	99.999	Marcasite	-152.314	99.999	Talc	18.615	18.619
Chrysotile	27.544	25.020	Sil. amorph.	-2.463	-3.200			

OREUSTOPNUN LINTONG.QUA
AUG.25

==========

S3 LINTONG

Program WATCH

Water sample (mg/kg)		Steam sample					
pH/deg.C	7.50/ 12.0	Gas (volume %)		Reference temperature	deg.C :	89.3	(Quartz)
CO2	152.20	CO2	.00				
H2S	.00	H2S	.00	Sampling pressure	bar abs. :	1.0	
NH3	.01	NH3	.00	Discharge enthalpy	kJ/kg :	374.	(Calculated)
B	.00	H2	.00	Discharge	kg/s :	4.0	
SiO2	38.30	O2	.00	Steam fraction at collection	:	.0000	
Na	187.30	CH4	.00				
K	8.40	N2	.00	Measured temperature	deg.C :	43.0	
Mg	3.600						
Ca	40.10	Liters gas per kg					
F	5.620	condensate/deg.C	.00/ .0	Condensate (mg/kg)			
Cl	128.70			pH/deg.C	.00/ .0		
SO4	217.60	Total steam (mg/kg)		CO2	.00		
Al	.010	CO2	.00	H2S	.00		
Fe	.010	H2S	.00	NH3	.00		
TDS	782.00	NH3	.00	Na	.00		

Ionic strength = .01416
Ionic balance : Cations (mol.eq.) .01044699 Anions (mol.eq.) .01145118 Difference (%) -9.17

Deep water components (mg/kg)				Deep steam (mg/kg)		Gas pressures (bars-abs.)	
B	.00	CO2	152.20	CO2	.00	CO2	.262E-01
SiO2	38.30	H2S	.00	H2S	.00	H2S	.000E+00
Na	187.30	NH3	.01	NH3	.00	NH3	.428E-07
K	8.40	H2	.00	H2	.00	H2	.000E+00
Mg	3.600	O2	.00	O2	.00	O2	.000E+00
Ca	40.10	CH4	.00	CH4	.00	CH4	.000E+00
F	5.620	N2	.00	N2	.00	N2	.000E+00
Cl	128.70					H2O	.683E+00
SO4	217.60					Total	.709E+00
Al	.0100						
Fe	.0100						
TDS	782.00	Aquifer steam fraction =	.0000				

Ionic strength = .01347 1000/T (Kelvin) = 2.76
Ionic balance : Cations (mol.eq.) .01009257 Anions (mol.eq.) .01109791 Difference (%) -9.49

Chemical geothermometers (degrees C)

Quartz	89.3	(Fournier & Potter, GRC Bulletin, pp. 3-12, Nov. 1982)
Chalcedony	58.0	(Fournier, Geothermics, vol. 5, pp. 41-50, 1977)
Na/K	124.4	(Arnorsson et al., Geochim. Cosmochim. Acta, vol. 47, pp. 567-577, 1983)

Oxidation potential (volts) : Eh H2S= 99.999 Eh CH4= 99.999 Eh H2= 99.999 Eh NH3= 99.999

Activity coefficients in deep water

H+	.891	KSO4-	.879	Fe++	.605	FeCl+	.873
OH-	.871	F-	.871	Fe+++	.356	Al+++	.356
H3SiO4-	.873	Cl-	.869	FeOH+	.877	AlOH++	.599
H2SiO4--	.599	Na+	.873	Fe(OH)3-	.877	Al(OH)2+	.879
H2BO3-	.867	K+	.869	Fe(OH)4--	.595	Al(OH)4-	.875
HCO3-	.873	Ca++	.605	Fe(OH)++	.595	AlSO4+	.875
CO3--	.590	Mg++	.623	Fe(OH)2+	.879	Al(SO4)2-	.875
HS-	.871	CaHCO3+	.881	Fe(OH)4-	.879	AlF++	.599
S--	.595	MgHCO3+	.873	FeSO4+	.877	AlF2+	.879
HSO4-	.875	CaOH+	.881	FeCl++	.595	AlF4-	.875
SO4--	.584	MgOH+	.883	FeCl2+	.877	AlF5--	.590
NaSO4-	.879	NH4+	.867	FeCl4-	.873	AlF6---	.305

Chemical species in deep water - ppm and log mole

Deep water pH is 7.322

H+	.00	-7.271	Mg++	2.09	-4.065	Fe(OH)3	.00	.000
OH-	.15	-5.054	NaCl	.22	-5.416	Fe(OH)4-	.00	.000
H4SiO4	59.88	-3.206	KCl	.00	-7.370	FeCl+	.00	-8.990
H3SiO4-	1.27	-4.875	NaSO4-	4.28	-4.445	FeCl2	.00	-22.742
H2SiO4--	.00	-8.429	KSO4-	.58	-5.371	FeCl++	.00	.000
NaH3SiO4	.12	-5.984	CaSO4	19.54	-3.843	FeCl2+	.00	.000
H3BO3	.00	.000	MgSO4	7.00	-4.236	FeCl3	.00	.000
H2BO3-	.00	.000	CaCO3	1.40	-4.856	FeCl4-	.00	.000
H2CO3	18.32	-3.530	MgCO3	.05	-6.260	FeSO4	.00	-7.712
HCO3-	186.22	-2.515	CaHCO3+	8.73	-4.064	FeSO4+	.00	.000
CO3--	.43	-5.142	MgHCO3+	.27	-5.500	Al+++	.00	-17.662
H2S	.00	.000	CaOH+	.01	-6.876	AlOH++	.00	-13.301
HS-	.00	.000	MgOH+	.01	-6.795	Al(OH)2+	.00	-9.451
S--	.00	.000	NH4OH	.01	-6.740	Al(OH)3	.01	-6.990
H2SO4	.00	-16.778	NH4+	.01	-6.392	Al(OH)4-	.05	-6.572
HSO4-	.00	-7.353	Fe++	.01	-6.923	AlSO4+	.00	-17.524
SO4--	194.37	-2.694	Fe+++	.00	.000	Al(SO4)2-	.00	-18.386
HF	.00	-7.174	FeOH+	.00	-7.410	AlF++	.00	-14.130
F-	5.62	-3.529	Fe(OH)2	.00	-9.447	AlF2+	.00	-11.958
Cl-	128.56	-2.441	Fe(OH)3-	.00	-12.855	AlF3	.00	-11.396
Na+	186.36	-2.091	Fe(OH)4--	.00	-18.394	AlF4-	.00	-12.468
K+	8.23	-3.677	Fe(OH)++	.00	.000	AlF5--	.00	-14.547
Ca++	30.32	-3.121	Fe(OH)2+	.00	.000	AlF6---	.00	-17.565

Log solubility products of minerals in deep water

	Theor.	Calc.		Theor.	Calc.		Theor.	Calc.
Adularia	-17.662	-19.843	Albite, low	-16.886	-18.255	Analcime	-13.499	-15.050
Anhydrite	-5.458	-6.267	Calcite	-9.261	-8.711	Chalcedony	-2.928	-3.206
Mg-Chlorite	-80.642	-84.859	Fluorite	-10.557	-10.518	Goethite	-5.066	99.999
Laumontite	-27.715	-29.139	Microcline	-19.116	-19.843	Magnetite	-30.517	99.999
Ca-Montmor.	-88.325	-103.337	K-Montmor.	-43.150	-53.736	Mg-Montmor.	-89.420	-104.268
Na-Montmor.	-43.124	-52.149	Muscovite	-21.825	-22.593	Prehnite	-37.170	-39.502
Pyrrhotite	-105.157	99.999	Pyrite	-154.905	99.999	Quartz	-3.205	-3.206
Wairakite	-25.008	-29.139	Wollastonite	11.163	8.098	Zoisite	-36.188	-40.877
Epidote	-44.473	99.999	Marcasite	-130.784	99.999	Talc	16.317	18.296
Chrysotile	24.557	24.707	Sil. amorph.	-2.276	-3.206			